JOURNAL OF GEOPHYSICAL RESEARCH, VOL. 104, NO. A12, PAGES 28,709-28,717, DECEMBER 1, 1999

Solitary potential structures associated with ion and electron beams near 1 R_E altitude

Scott R. Bounds,[1,2] Robert F. Pfaff,[1] Stephen F. Knowlton,[3] Forrest S. Mozer,[4] Michael A. Temerin,[4] and Craig A. Kletzing[5]

Abstract. Small-scale solitary electric potential structures are commonly observed on auroral field lines with the Polar Electric Field Instrument (EFI). This study focuses on observations of solitary structures in the southern hemisphere auroral zone at altitudes between 5500 and 7500 km. Some of the potential structures are similar to those observed previously by the S3-3 and Viking satellites and are inferred to be negative potential pulses traveling upward along the auroral magnetic field lines, associated with upgoing ion beams and upward currents. The velocities of these "ion" solitary potential structures are estimated, using spaced EFI measurements, to be distributed within the range of ~75 - 300 km s^{-1}. In addition to these structures, a different type of solitary potential structure with opposite polarity has been observed with faster propagation velocities. These faster structures (termed "electron" solitary potential structures) are distinguishable from the slower, ion solitary structures in that their distinctive bipolar electric field signature, common to both types of solitary structure, is reversed. The ultimate distinction for the electron solitary potential structures is that they are observed on auroral field lines in conjunction with magnetically field-aligned upflowing electron beams. The electron solitary potential structures propagate up the field line in the same direction as the electron beam. An example is shown of the polarity reversal from ion to electron solitary potential structures coincident with a simultaneous shift from upgoing ion beams to upgoing electron beams.

1. Introduction

There have been numerous observations of small-scale (temporal and spatial), large-amplitude, magnetic field-aligned electric fields in the auroral acceleration region [e.g., *Temerin et al.*, 1982, *Boström et al.*, 1988; *Mozer et al.*, 1997; *Ergun et al.*, 1998]. These structures have been commonly called solitary waves or weak doubles layers and appear to be prevalent throughout many parts of the magnetosphere. For instance, they have been reported in the plasma sheet boundary layer by the Geotail satellite [*Matsumoto*, 1994], by the Plasma Wave Instrument on the Polar satellite (2 to 8.5 R_E radial distance) [*Franz et al*, 1998; *Tsurutani et al*, 1998], and by the Electric Field Instrument (EFI) on the Polar satellite (~ 4 to 7 R_E radial distance) [*Cattell et al.*, 1999]. *Cattell et al.* [1999] also report observation of solitary potential structures in the high-altitude cusp region (~5 to 9 R_E radial distance). In this article, we focus only on the structures observed by Polar EFI during perigee passes of the Polar satellite near 1 R_E altitude in the southern auroral zone.

[1]NASA Goddard Space Flight Center, Greenbelt, Maryland.
[2]Now at Department of Physics and Astronomy, University of Iowa, Iowa City.
[3]Physics Department, Auburn University, Auburn, Alabama.
[4]Space Sciences Laboratory, University of California at Berkeley, Berkeley.
[5]Department of Physics and Astronomy, University of Iowa, Iowa City.

Paper number 1999JA900284.
0148-0227/99/1999JA900284$09.00

Solitary structures are identified in satellite electric field measurements by their signature of bipolar electric field fluctuations of short duration oriented predominantly parallel to the magnetic field. The electric fields associated with the structures typically have measured amplitudes around 50 to 150 mV m^{-1} [e.g., *Mozer et al.*, 1997] parallel to the magnetic field. The structures were first observed in the auroral acceleration region in S3-3 satellite data by *Temerin et al.* [1982]. Measurements gathered using the S3-3 electric field instrument suggest that solitary structures most likely are negative potential pulses propagating up the field line, past the spacecraft, with estimated velocities greater than 50 km s^{-1} parallel to the magnetic field. Given this velocity magnitude, the typical width of the solitary structure along the magnetic field direction was inferred to be 300 m. Furthermore, the structures were observed at altitudes ranging from 6000 to 8000 km and were co-located with upward flowing ion beams and electrostatic ion cyclotron wave activity [*Temerin et al.*, 1982].

Further observations of solitary structures were gathered by the Viking satellite [*Boström et al.*, 1988; 1989; *Koskinen et al.*, 1990]. The Viking satellite's spherical sensors were operated in a Langmuir probe mode to measure ion density. The solitary structures were found to represent localized density depletions. By measuring the time delay between the density depletion signatures measured by two probes separated by 80 m in the spin plane of that satellite, the solitary structures were determined to be propagating between 5 and 50 km s^{-1} upward along the magnetic field direction. These velocities implied parallel widths of 100 - 300 m. The accuracy of these velocity measurements has recently been reexamined [*Eriksson et al.*, 1997; *McFadden*, 1998]. As in the S3-3 study, the occurrences of solitary

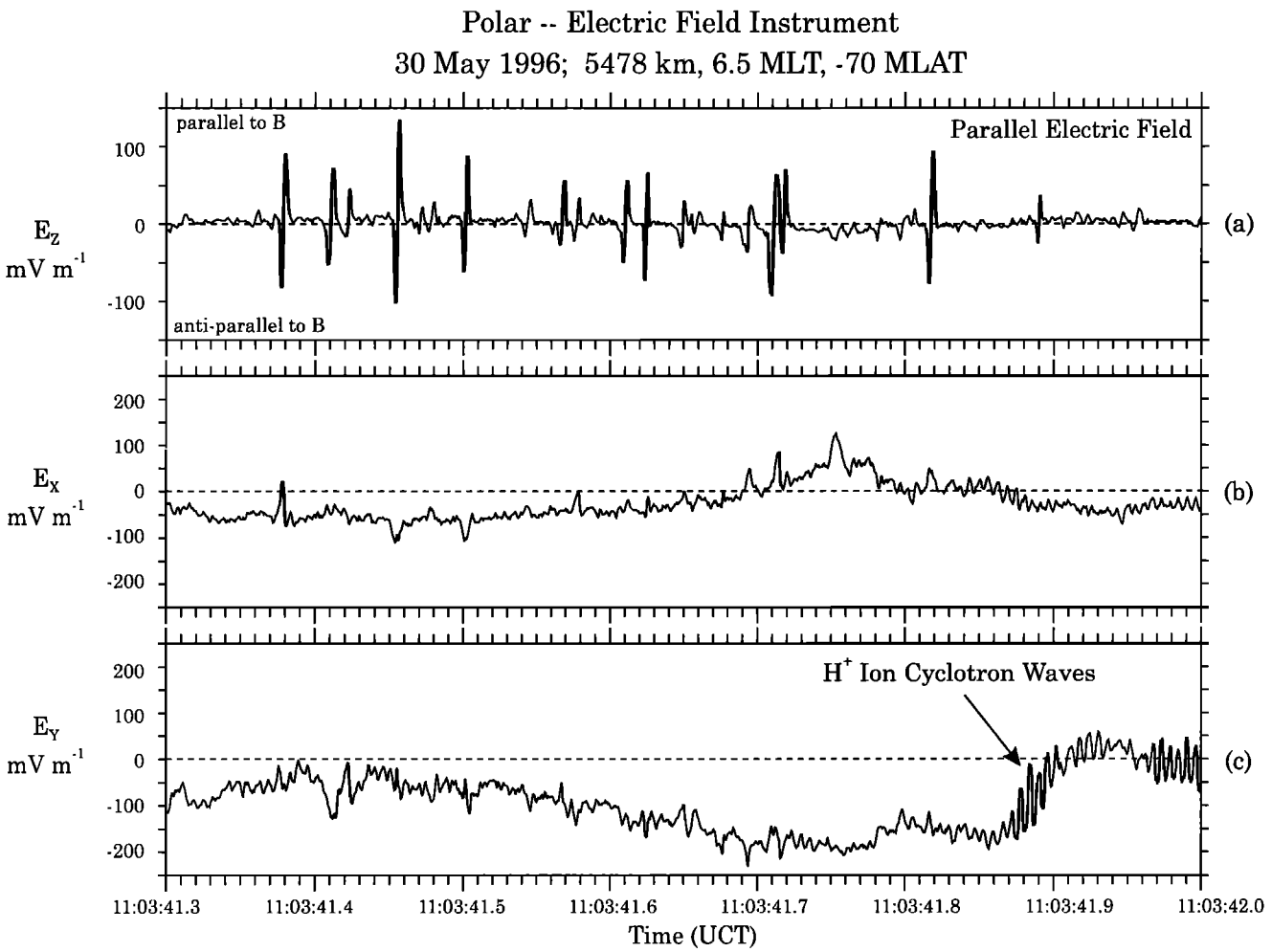

Figure 1. Electric field observations in field-aligned current coordinates showing multiple solitary potential structures over a period of 0.7 s. Here E_Z is along the magnetic field direction, E_X is perpendicular to E_Z and pointing toward the equatorial plane of the Earth, and E_Y is orthogonal to E_X and E_Z and completes the three axis Cartesian coordinates. The electric field components perpendicular to the magnetic field include slowly-varying $V_{sc} \times B$ contributions due to the satellite's motion perpendicular to the magnetic field.

structures observed with the Viking probes were correlated with upflowing ion beams.

Despite the numerous observations of solitary structures, several unanswered questions concerning this phenomenon remain. For example, the growth mechanism for these large-amplitude potential structures, for which $\Phi_0 \geq kT_e/e$, where Φ_0 is the maximum amplitude of the potential associated with the solitary structure and T_e is the ambient electron temperature, has yet to be completely understood [*Mälkki et al.*, 1989]. The role these structures play in the auroral acceleration process, if any, and how they are formed have yet to be determined. Such questions provided motivation for the present study.

2. Polar Instrumentation Relevant to this Study

The data used in this study were gathered with the Polar satellite Electric Field Instrument (EFI), which consists of four spherical sensors on the ends of 100 and 130 m (tip-to-tip) wire boom pairs in the spin plane, and two spherical sensors on shorter (13.5 m tip-to-tip) semi-rigid booms along the spin axis of the spacecraft which provide the third axis measurement [*Harvey et al.*, 1995]. During perigee passes in the southern auroral region, the direction of the magnetic field vector typically lies within ~10° of the satellite spin plane, and in such cases, the wire boom spin plane probes alone can be used to obtain the electric field component parallel to the magnetic field with high confidence. The present study focuses on selected low altitude (5500 to 7500 km) southern auroral zone passes between May 14, 1996, and December 31, 1997.

As will be shown below in detail, the electric field signatures corresponding to the solitary structures observed in this study have time signatures ranging from 2 to 10 ms. Fast-time scale fluctuations such as these solitary structures are only resolved when the dc-coupled electric field waveform is obtained when EFI is operating in its burst mode in which the data-sampling rate is either 1600 samples per second or 8000 samples second. (Note that the nonburst or "survey" sampling rate for EFI, 40 samples per second, is generally insufficient to resolve even the slowest solitary potential structures.) Given onboard memory constraints, the 1600 samples-per-second burst mode is limited to two data periods of 30 s each approximately once per orbit, whereas the EFI burst mode of 8000 samples per second occurs considerably less frequently. When such data are acquired, the velocity may be calculated by comparing time shifts between spatially separated

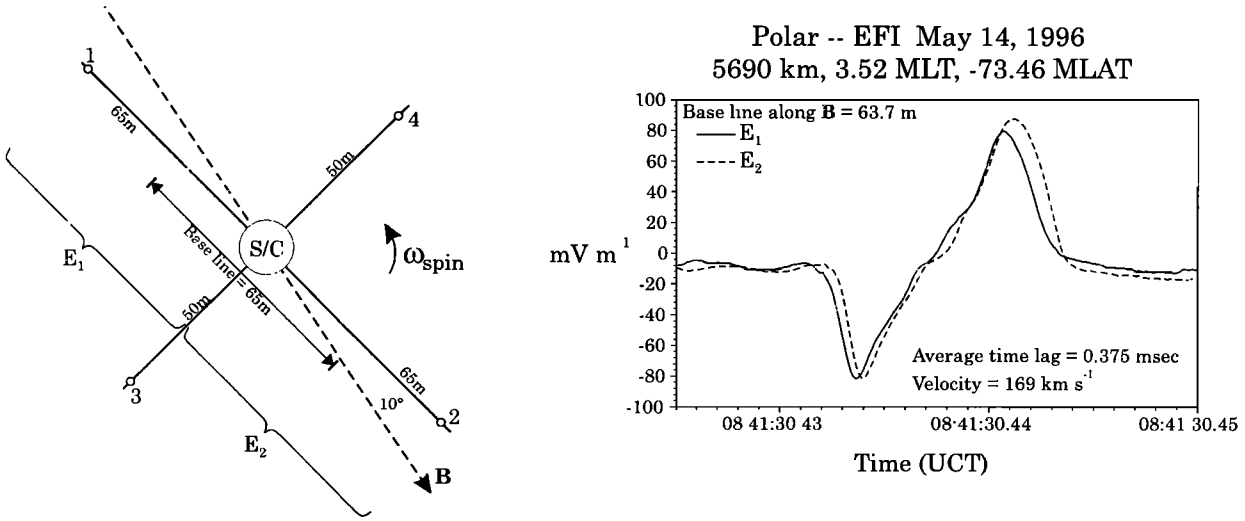

Figure 2. Spaced receiver measurement geometry is shown on the left. The time lag between the E_1 and E_2 measurements of a solitary potential structure and the corresponding velocity parallel to the magnetic field are shown in the panel on the right. The data were collected at 8000 samples per second.

double probes, which consist of opposing spheres and the average of the orthogonal spin plane probe pair potentials.

This study also utilizes ion and electron particle distributions between 100 eV and 20 keV energy recorded by the Hydra particle spectrometer onboard Polar [*Scudder et al.*, 1995]. The magnetic field direction and local currents were inferred using the Magnetic Field Experiment (MFE) fluxgate magnetometer [*Russell et al.*, 1995].

3. Solitary Potential Structures Associated With Ion Beams

An example of solitary structures observed in the southern auroral zone near 1 R_E altitude by EFI is shown in Figure 1, which displays the electric field components parallel and perpendicular to the magnetic field. Notice that the distinctive bipolar parallel electric field signatures of multiple solitary structures are the dominant electric field signature, as seen in Figure 1a. The structures sometimes have unipolar perpendicular electric fields associated with them, as shown in Figure 1b, although it is difficult to distinguish them in this figure. The fluctuations superimposed on the perpendicular dc level are geophysical electric fields with a characteristic period of 10 ms corresponding to the local hydrogen cyclotron period. Observations of such perpendicular ion cyclotron waves coincident with regions of parallel solitary structures in the acceleration region have been reported by *Temerin et al.* [1982].

The velocity of the structures is determined using the spaced double-probe technique, for which an example is shown in Figure 2 using 8000 sample s^{-1} burst data. In this procedure, the time shift between measurements of the electric field detected between each individual opposing sphere and the average potential at the central spacecraft location are carried out. Using the separation baseline of 50 or 65 m (depending on which boom pair is used) which thus corresponds to the midpoints of the respective separated pair of measurements, the components of the velocity along the direction of each measurement pair are obtained. The baseline distance is adjusted for the angle between the probe pairs and the magnetic field, although the solitary structures events studied here are intentionally chosen such that this angle is small and therefore the adjustment is minimal. The example shown in Figure 2 yields a propagation velocity of ~170 km s^{-1}, which we find is typical of this type of structure. Although not shown here, the solitary structures in Figures 1 and 2 are each associated with upflowing ion beams and are similar to the solitary structures reported in the data from the S3-3 and Viking satellites [e.g. *Temerin et al.*, 1982; *Boström et al.*, 1988]. We thus refer to such solitary structures as ion solitary structures.

We have also examined in detail cases where multiple solitary structures are observed over several consecutive spins of the spacecraft. In these cases, the correlation analysis shows that at the times where the spaced receivers are aligned closely to the magnetic field direction, the structures are clearly evident in both pairs of receivers. Here a clear and measurable time lag is present, such that the derived structure velocity is consistently in the direction of the upflowing ion beam as mentioned above. As the spacecraft spins so that the same pair of receivers is perpendicular to the magnetic field, the characteristic bipolar signature of the structure is not evident and no cross correlation is calculated. In fact, when the receivers are perpendicular to the magnetic field, the detectors typically observe unipolar pulses associated with the flanks of the structure. These unipolar pulses have no discernable time lag between spaced receivers. As the receivers rotate to an antiparallel orientation with respect to the magnetic field, the signatures become clear again and the cross-correlation analysis demonstrates that the velocities remain in the direction of the ion beam. This behavior supports the fact that the structures reported here are likely geophysical phenomenon associated with the ion beam rather than effects produced by the spacecraft.

A cross-correlation analysis of more than 100 examples of ion solitary structures observed by EFI in the auroral acceleration region has determined the velocities to be predominantly in the range of 75 - 300 km s^{-1} and parallel to the magnetic field direction, traveling anti-earthward or up the magnetic field line. This differs from previous satellite measurements (< 50 km s^{-1}) which suggest that these structures move in phase with the background plasma [*Boström et al.*, 1988, 1989; *Koskinen et al.*,

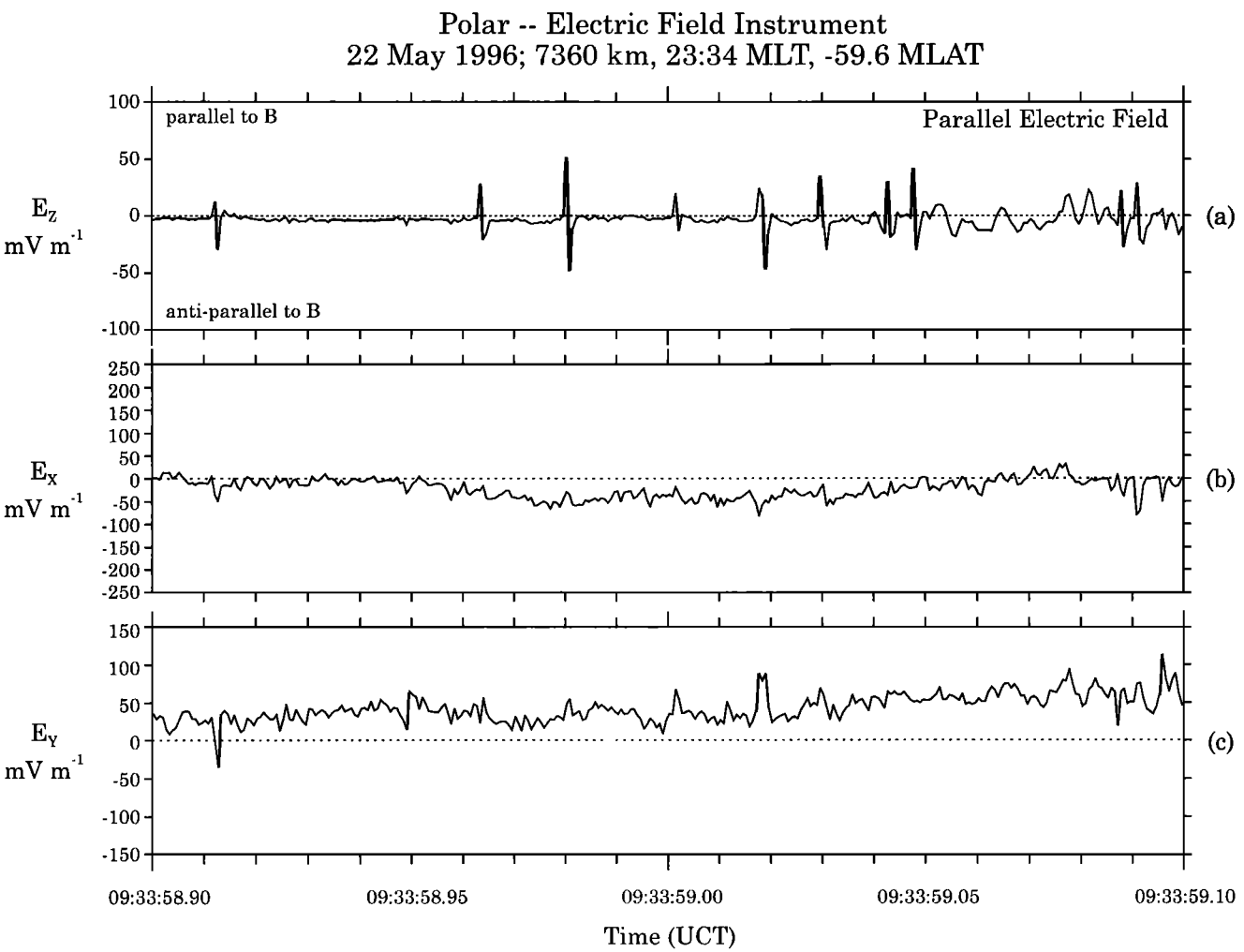

Figure 3. An example of electron solitary potential structures for a 0.2 s time interval. Notice the reverse polarity of the structures in panel (a) compared to those in Figure 1a (coordinate system is same as in Figure 1.). Since the solitary potential structure waveforms are only marginally sampled at 1600 samples s^{-1}, they may under represent the true amplitudes of the peaks in the signal.

1990]. The velocities reported here suggest the structures move in phase with the ion beams. Taking an example on May 14, 1996 (Figure 2), in which the highest resolution sampling of a few solitary structures was obtained, the particle data from the Hydra instrument (not shown) revealed upflowing ion beams with peak energy between 300 to 500 eV. Assuming, for the purposes of the discussion here that these ions are perfectly field-aligned, these energies infer ion beam velocities for H^+ of the order of 250 to 300 km s^{-1} and for O^+ of the order of 60 to 75 km s^{-1}. The solitary structure velocities measured during this period are between 120 and 250 km s^{-1}, which is located between the peaks of the two ion beam distributions.

4. Solitary Potential Structures Associated With Electron Beams

An example of a different type of solitary potential structure is shown in Figure 3. Notice immediately that the order of the "positive then negative" electric fields of the bipolar signature in these events is reversed, with respect to time, compared to those in Figure 1. Similar small timescale parallel electric field structures with such opposite polarity were also observed in the Polar EFI data in the auroral zone by *Mozer et al.* [1997] and by *Ergun et al.* [1998] using electric field data from the FAST satellite. *Ergun et al.* [1998] termed them "fast" solitary potential structures to distinguish them from the previously observed, slower solitary potential structures. The amplitudes of the electron solitary potential structures ($E_{max} \leq 100$ mV m^{-1}) in Figure 3a are in general much less than the electron solitary potential structure amplitudes ($E_{max} \leq 2.5$ V m^{-1}) reported by *Ergun et al.* [1998] using the FAST data set. It is unclear why this is the case, but it might be related to the obvious undersampling of the structures by EFI, whereas the FAST electric field experiment is specifically designed for higher sampling rates. Note that the polarity of the structures shown in Figure 3a are reversed from that in Figure 3 of *Ergun et al.* [1998] since the two data sets were gathered in opposite hemispheres and the magnetic field direction is reversed between the two data sets. In other words, both data sets show positive potential pulses moving anti-earthward in the electron beam direction, as will be shown below.

The fast solitary potential structure events have a shorter timescale than the normal solitary potential structures and are undersampled at a data acquisition rate of 1600 samples per

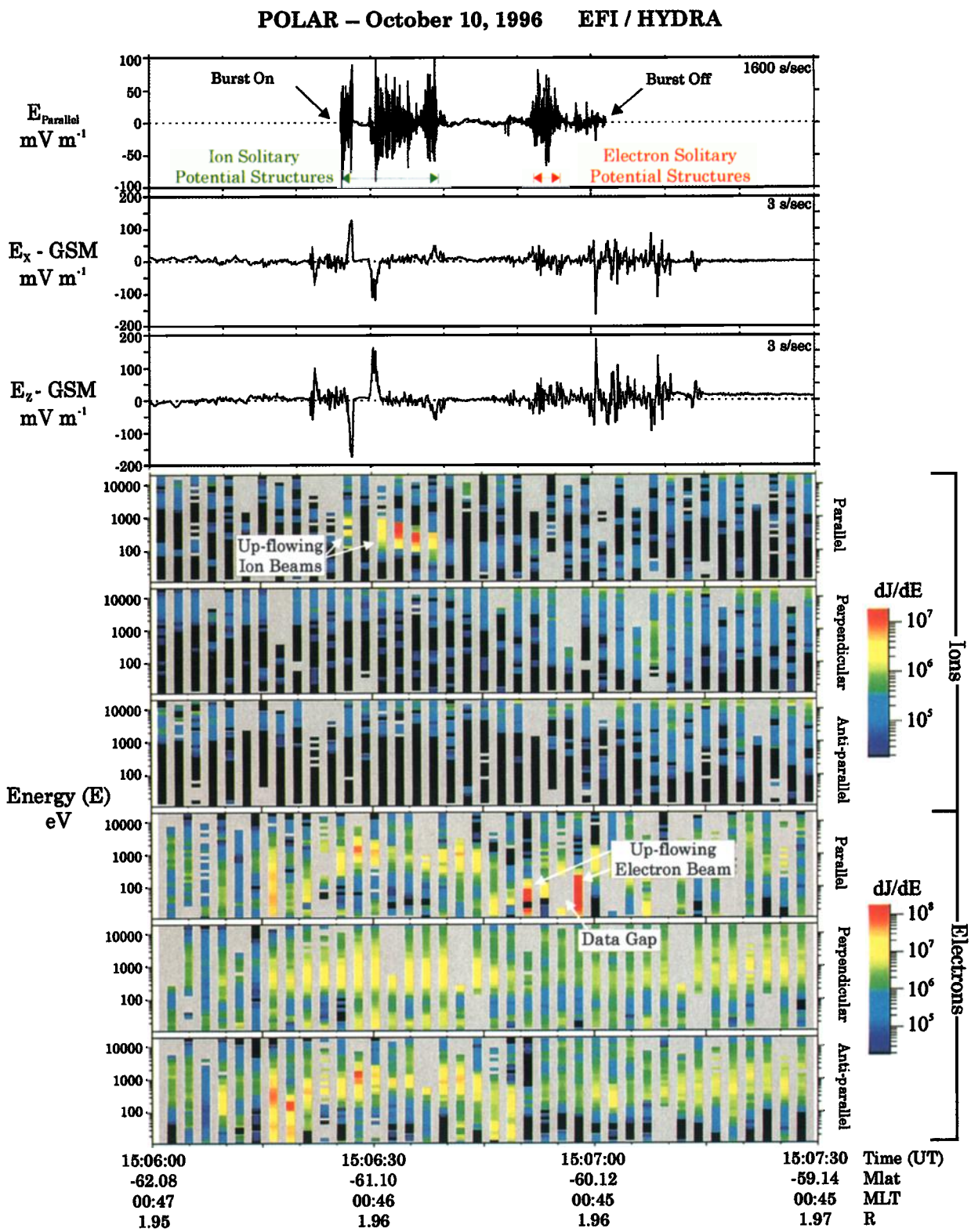

Plate 1. Electric Field Instrument (EFI) and Hydra data for a Southern Hemisphere auroral zone pass on October 10, 1996. (top) These data show the particle environment for both ion and electron solitary potential structures captured in a single EFI burst packet. Upflowing ion beams can clearly be seen in the region of ion solitary potential structures and upflowing electron beams are observed in the region of fast or electron solitary potential structures. Strong perpendicular electrostatic shocks (seen in E_X-GSM and E_Z-GSM coordinates, where GSM is Geocentric Solar Magnetospheric system) are observed on the flanks of the region where both the ion beam and solitary potential structures disappear for a brief period.

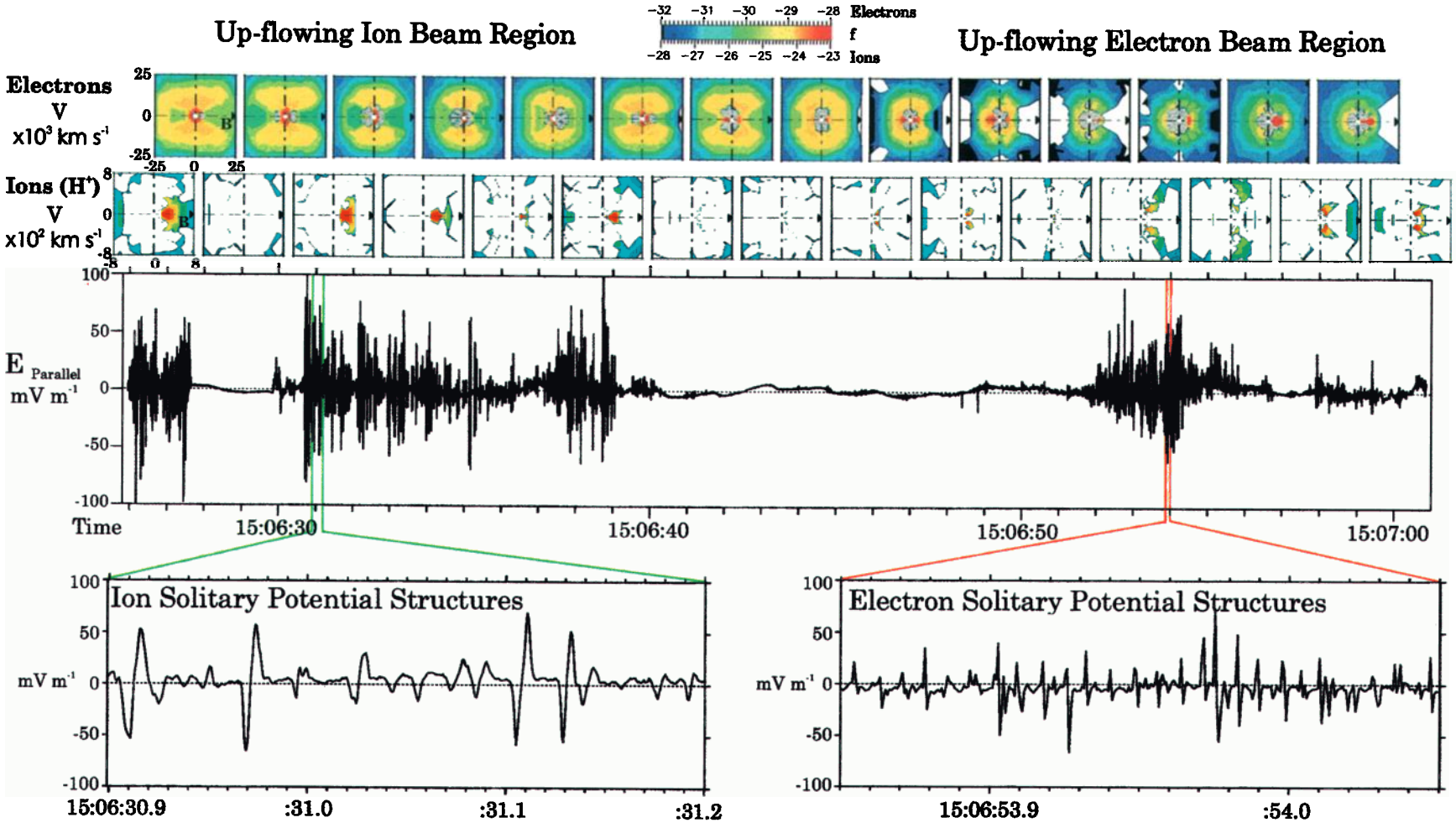

Plate 2. Time evolution of the ion and electron particle distributions with respect to contiguous observations of the parallel electric fields which include ion and electron solitary potential structures on October 10, 1996. The strong correlation of solitary potential structures and upflowing ion beams can clearly be seen in the first half of the data. In the ion solitary potential structure region, electrons display a loss cone type distribution and the ions display a strong anti-earthward parallel acceleration. The second half shows the distributions in a region of electron solitary potential structures. Here the total electron population is colder and does not show distinct loss cone features, whereas the ions show conic distributions. The electrons show anti-earthward directed beams accelerated parallel to the magnetic field.

second, making an accurate determination of both their amplitude and velocity difficult in the Polar EFI data set. The 1600 sample per second data show barely measurable velocity magnitudes implying that their minimum propagation velocity is much greater than those of the ion solitary potential structures. Furthermore, the velocities of fast solitary potential structures reported by *Ergun et al.* [1998] are between 500 and 5000 km s^{-1}. *Franz et al.* [1998] and *Cattell et al.* [1999] report velocities of the order of 1000 km s^{-1}.

The fast, reverse polarity solitary potential structures observed here were associated with electron beams. Other such structures observed in the auroral acceleration were also associated with electron beams [e.g., *Ergun et al.*, 1998]. We hence refer to this type of structure as electron solitary potential structures. We now show an example of both ion and electron solitary potential structures captured in the same burst event by the Polar electric field instrument. Included in this example is the energetic particle environment in which the two types of solitary potential structures are observed.

5. Relation of Solitary Potential Structures to Energetic Ion and Electron Beams

An energy spectrogram of parallel and perpendicular ion and electron distributions obtained in a southern auroral pass on October 10, 1996, is shown in Plate 1. Ion and electron solitary potential structures observed by EFI during this interval are shown in the upper panels. Notice that ion solitary potential structures occur only in the presence of upflowing ion beams which are shown to have typical energies E_b = 0.1 - 1 keV. In this case, the peak energy is ~0.4 keV. The presence of the ion solitary potential structures also correlates with a region of upward current as inferred from the gradients in the flux gate magnetometer data (not shown).

Approximately 20 s later, an intense upgoing electron beam is observed. Coincident with this beam, fast or electron solitary potential structures, distinguishable by their opposite polarity, were observed. Although we cannot determine their propagation velocity in this example, we assume that these structures are similar to those reported by *Ergun et al.* [1998] and that they also propagate along the magnetic field line away from the Earth. The propagation direction for both species is thus dictated by the beam direction with which each species of solitary potential structure is associated: ion solitary potential structures propagate with the ion beam and electron solitary potential structures propagate with the electron beam.

The correlation of these beams and solitary potential structures is shown in more detail in Plate 2, in which 35 s of EFI burst data parallel to the magnetic field are displayed alongside the time evolution of the measured energetic electron and ion distributions. The first half of the burst shows multiple, slow ion solitary potential structures and the ion beam associated with them, whereas the second half of the figure shows the switch to an upflowing electron beam with a coincident group of fast electron solitary potential structures.

Plates 1 and 2 both reveal a quiescent period in the observation of ion solitary potential structure signatures at 1506:28 - 1506:30 UT, which is precisely where the observed ion beam also disappears. This observation thus reinforces a strong dependence of the ion solitary potential structures on the existence of the ion beams. The presence of simultaneous downward electrons at the same time suggests that the ion solitary potential structures may be present in regions of a large-scale upward parallel electric field. Notice also that there exist large perpendicular fields (or "shocks") near 1506:28UT. In Plate 1, the shocks are oriented in opposite directions on either side of the gap. These are interpreted as two nearly adjacent regions of converging electric fields associated with the parallel potential which could be accelerating the ions below the satellite [see *McFadden et al.*, 1998, and references therein]. Subsequently, it is theorized that nonlinearities associated with instabilities in the ion beam may produce the solitary potential structures.

The fact that the fast electron solitary potential structures are observed in close proximity to the slower ion solitary potential structures as shown in Plates 1 and 2 is clearly a result of the switch from an ion beam to an electron beam plasma environment. Although the amplitudes of the structures are similar in this example, at first glance undersampling of the solitary potential structures, particularly for the election solitary potential structures, suggests that larger amplitudes may be present. However, given the large number of electron solitary potential structures detected in this sample, it is unlikely that their amplitudes were considerably larger than those presented here or else some of the spikes would be expected to show larger amplitudes. The electron solitary potential structures appear to be somewhat less correlated with the upflowing electron beam in this example although the data gap in the electron data at 1506:55UT may mask some of the expected correlation. In all examples studied to date, electron solitary potential structures are always observed in the presence of electron beams. Notice further in Plate 2 that the electron solitary potential structures are also observed in the presence of ion conics.

6. Discussion and Conclusions

The bipolar electric field of the ion solitary structures indicates that the electric potential of the structure is a unitary pulse of finite amplitude with little or no net potential drop across the structure. A simple representation of each structure is shown in Figure 4. In the case of the ion solitary structures, the electric field may be considered convergent from the center of the structure. In the case of the electron solitary potential structures, the electric field may be considered to be divergent from the center of the structure. As structures quickly pass the relatively stationary satellite, a bipolar signature is produced in the electric field component along the propagation direction. The electric field component perpendicular to the direction of propagation would produce a unipolar signature. This unipolar electric field could be either negative or positive depending on which side the satellite is relative to the structure. (If the satellite were positioned near the center of the structure, no clear signature would be detected in the perpendicular component.) The data shown in Figures 1 and 3 support this interpretation.

Given the observed propagation directions and the measured electric fields reported here, these structures have very similar potential signatures as those reported by previous researchers. The ion solitary potential structures are negative potential pulses or ion holes [*Boström et al.*, 1988; *Mälkki et al.*, 1989; *Koskinen and Mälkki*, 1993] and the electron solitary potential structures are positive potential pulses or electron holes [*Matsumoto et al.*, 1994; *Ergun et al.*, 1998; *Franz et al.*, 1998; *Cattell et al.*, 1999; *Tsurutani et al.*, 1998].

Using a similar analysis as described by *Mälkki et al.* [1989], we assume a simple model for the potential pulse moving along

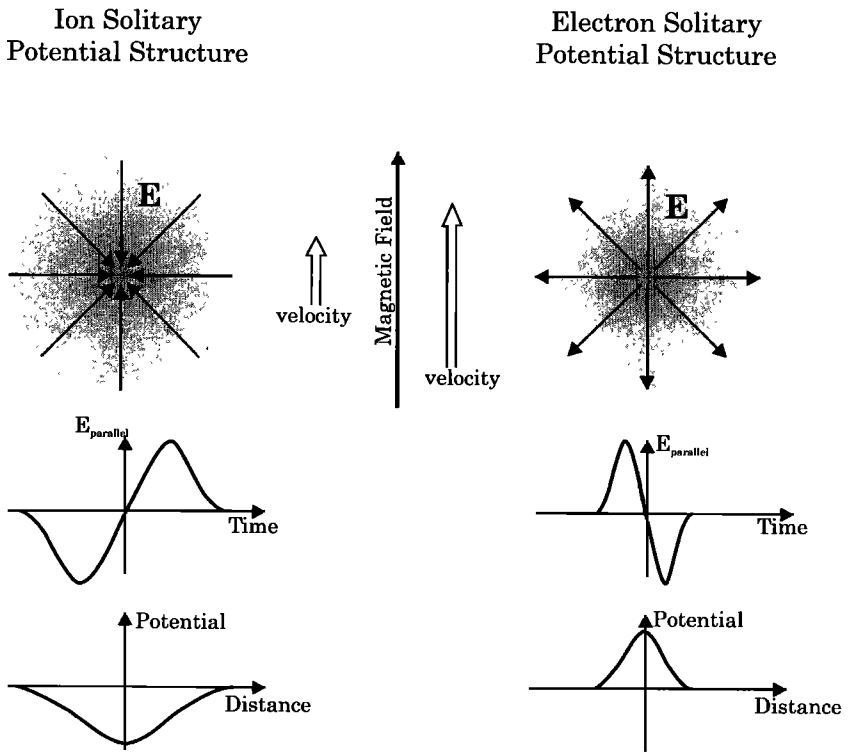

Figure 4. Simple model showing the convergent electric fields (left) of the ion solitary potential structure and the divergent electric fields (right) of the electron solitary potential structure. The middle illustrations show sketches of the measured electric fields as the solitary potential wells move past the relatively stationary satellite. The inferred potentials corresponding to these electric field measurements are sketched below in the lowest illustrations.

the magnetic field line with a functional form given by $\Phi(x) = \Phi_0$ sech^2 $[(x\text{-}vt)/l]$. The velocity measurements can be used to infer the potential amplitude, Φ_0, and scale width, l, of the structure. Using this technique for the ion solitary structures similar to those shown in Figure 2 with a peak electric field of 50 mV m^{-1} and a velocity of 165 m s^{-1}, the physical widths of such structures are determined to be ~1.5 km in the direction parallel to the magnetic field, with potential amplitudes of the order of -30 V. These widths are considerably greater than the Debye length, λ_{DE} ~ 20 to 100 m determined using Hydra measurements of the electron temperature for the case on May 14, 1996. We note that the measurement of electron temperature in this region is uncertain because the distributions are non-Maxwellian. Using this same model and assuming a propagation velocity of 1000 km s^{-1}, the physical size of the electron solitary structures with a peak electric field amplitude of 50 mV m^{-1} is of the order of 800 m with a peak potential of ~12 V.

Observations of ion solitary structures by the Electric Field Instrument on the Polar satellite are similar to previous examples of such features as observed by electric field and plasma density probes on previous satellites in the auroral zone [*Temerin et al.*, 1982; *Boström et al.*, 1988]. In agreement with previous observations, these structures are correlated with upflowing ion beams in regions of upward currents. However, the velocities of the ion solitary potential structures reported here are different from those measured by previous studies. Our study infers velocities in the range of 75 - 300 km s^{-1}, whereas Viking measured velocities in the range of 5 - 50 km s^{-1} [*Boström et al.*, 1988]. From S3-3 satellite data, the velocities were estimated to be ≥ 50 km s^{-1} [*Temerin et al.*, 1982]. The higher measured velocities that we report here have two important consequences.

The first consequence is that the higher velocities of the ion solitary structures infer different measurements for the potential amplitude, Φ_0, and physical size, L, of the structures as estimated above. Whereas measurements gathered by the probes on the Viking satellite were used to estimate potential amplitudes smaller than those corresponding to the ambient electron temperature ($\Phi_0 \sim 0.5\ kT_e/e$), the propagation velocity measurements of ion solitary structures reported here yield broader estimates of the structures, $L_{||} \geq 1.5$ km, with potential amplitudes of the order of, or larger than, those corresponding to the ambient electron temperature ($\Phi_0 \sim kT_e/e$).

The second consequence of the faster ion solitary structures is relevant to with which ion population the structures are resonant [*Mälkki et al.*, 1989; *Koskinen and Mälkki*, 1993]. Given the measured velocities of 5 - 50 km s^{-1} as measured by Viking, the structures were assumed to be propagating at speeds which are in phase with the velocities of ions in a cold background distribution. A number of theories have been put forward to explain the growth of the structures in a background ion population. This growth can be excited by the injection of an ion beam [*Tetreault*, 1988; *Gray et al.*, 1991; *Marchenko and Hudson*, 1995]. However, the faster Polar velocity measurements, 75 - 300 km s^{-1}, suggest the structures propagate in phase with the observed ion beams or perhaps within the overlap region between O^+ and H^+ beam distribution and/or the rising edge of the H^+ beam population. This result suggests that the solitary structures are possibly the nonlinear consequence of an ion acoustic wave growth from the two-stream instability of the two ion species [*Bergmann and Lotko*, 1986]. The structures would be produced in a similar fashion as discussed by *Gray et al.* [1991] and *Marchenko and Hudson* [1995] except that in

those simulations the background plasma would be replaced by the O^+ beam. Such a growth mechanism would not require a cold background ion population which is conjectured not to exist in the acceleration region [*McFadden et al.*, 1998].

Regarding the electron solitary structures, the data presented here and in other references support their clear association with electron beams, with considerably faster speeds, and with spatial potential wells of opposite polarity to that of the ion solitary structure. Unfortunately, because of undersampling, analysis of the electron solitary potential structure velocity in the Polar EFI data is limited. Data from the Polar/PWI instrument are sampled at a much higher rate and thus provide a more adequate measurement of the electron solitary structure velocities [*Franz et al.*, 1998]. Future studies that combine the Polar EFI, PWI, Hydra, and TIMAS data over a wide range of altitudes (1-3 R_E) in the auroral acceleration region and relate the solitary structure amplitudes and velocities to the electron beam characteristics promise to advance our understanding of the relationship of beams and solitary structures by a large degree.

Acknowledgments. We thank Chris Russell and the MFE team for providing magnetic field data used by both the EFI and Hydra teams. H. Freudenreich provided assistance with the phase velocity analysis. This research was initiated during a stay by one of us (S.B.) at the Goddard Space Flight Center during the summer 1996 funded by a NASA Alabama Space Grant Fellowship and has been supported by the NASA Goddard Space Flight Center since Summer 1997 using the Polar EFI Research Grant to Goddard. This work was also performed under NASA grant number NAG 5 2231 and DARA grant 50 OC 8911 0. The results of the Hydra investigation were made possible by the hardware efforts of groups led at NASA GSFC by K. Ogilvie, at UNH by R. Torbert, at MPAe by A. Korth, and UCSD by W. Fillius.

Janet G. Luhmann thanks the referees for their assistance in evaluating this paper.

References

Bergmann, R., and W. Lotko, Transition to unstable ion flow in parallel electric fields, *J. Geophys. Res.*, *91*, 7033-7045, 1986.

Boström, R., G. Gustafsson, B. Holback, G. Holmgren, H Koskinen, and P. Kintner, Characteristics of solitary waves and weak double layers in the magnetospheric plasma, *Phys. Rev. Lett.*, *61*, 82, 1988.

Boström, R., B. Holback, G. Holmgren, and H. Koskinen, Solitary structures in the magnetospheric plasma observed by Viking, *Phys. Scr.*, *39*, 782, 1989.

Cattell, C. , J. Dombeck, J. R. Wygant, M. K. Hudson, F. S. Mozer, M A. Temerin, W. K. Peterson, C. A. Kletzing, C. T. Russell, and R. F. Pfaff, Comparisons of Polar satellite observations of solitary wave velocities in the plasma sheet boundary and the high-altitude cusp to those in the auroral zone, *Geophys. Res. Lett.*, *26*, 425-428, 1999.

Ergun, R. E. et al., FAST satellite observations of large-amplitude solitary structures, *Geophys. Res. Lett.*, *25*, 2041-2044, 1998.

Eriksson, A. I., A. Mälkki, P. O. Dovner, R. Boström, G. Holmgren, and B. Holback, A statistical survey of auroral solitary waves and weak double layers, 2; Measurement accuracy and ambient plasma density, *J. Geophys. Res.*, *102*, 11385-11398, 1997.

Franz, J. R., P. M. Kintner, and J. S. Pickett, Polar observation of coherent electric field structures, *Geophys. Res. Lett.*, *25*, 1277-1280, 1998.

Gray, P. C., M. K. Hudson, W. Lotko, and R. Bergmann, Decay of ion beam driven acoustic waves into ion holes, *Geophys. Res. Lett.*, *18*, 1675-1678, 1991.

Harvey, P. et al., The electric field instrument on the Polar satellite, *Space Sci. Rev.*, *71*, 583-596, 1995.

Koskinen, H. E. J., and A. Mälkki, Auroral weak double layers: A critical assessment, in *Auroral Plasma Dynamics*, *Geophys. Monogr. Ser.*, vol. 80, edited by R. L. Lysak, pp. 97-104, AGU, Washington, D.C., 1993.

Koskinen, H. , R. Lundin, and B. Holback, On the plasma environment of solitary waves and weak double layers, *J. Geophys Res.*, *95*, 5921, 1990.

Mälkki, A., H. Koskinen, R. Boström, and B. Holback, On theories attempting to explain observations of solitary waves and weak double layers in the auroral magnetosphere, *Phys. Scr.*, *39*, 787-793, 1989.

Marchenko, V. A., and M. K. Hudson, Beam-driven acoustic solitary waves in the auroral acceleration region, *J. Geophys. Res.*, *100*, 19791, 1995.

Matsumoto, H., H. Kojima, T. Miyatake, Y. Omura, M. Okada, I. Nagano, and M. Tsutsui., Electrostatic Solitary Waves (ESW) in the magnetotail: BEN wave forms observed by GEOTAIL, *Geophys. Res. Lett.*, *21*, 2915, 1994.

McFadden, J. P., What is known and unknown about particle acceleration of auroral field lines, *Eos Trans. AGU*, 79. (17), Spring Meet. Suppl., S316, 1998.

McFadden, J. P., et al., Spatial structure and gradients of ion beams observed by FAST, *Geophys. Res. Lett.*, *25*, 2021-2024, 1998.

Mozer, F. S., R. Ergun, M. Temerin, C. Cattell, J. Dombeck, and J. Wygant, New features of time domain electric field structures in the auroral acceleration region, *Phys. Rev. Lett.*, *79*, 1281, 1997.

Russell, C. T., R. C. Snare, J. D. Means, D. Pierce, D. Dearborn, M. Larson, G. Barr, and G. Le, The GGS/Polar Magnetic Fields Investigation, *Space Sci. Rev.*, *71*, 563-582, 1995.

Scudder, J., F. et al., HYDRA - A 3-dimensional electron and ion hot plasma instrument for the Polar spacecraft of the GGS mission, *Space Sci. Rev.*, *71*, 459-495, 1995.

Temerin, M., K. Cerny, W. Lotko, and F. S. Mozer, Observations of double layers and solitary waves in the auroral plasma, *Phys. Rev. Lett.*, *48*, 1175, 1982.

Tetreault, D. J., Growing ion holes as the cause of auroral double layers, *Geophys. Res. Lett.*, *15*, 164-167, 1988.

Tsurutani, B. T., J. K. Arballo, G. S. Laknina, C. M. Ho, B. Buti, J. S. Pickett, and D. A. Gurnett, Plasma waves in the dayside polar cap boundary layer: Bipolar and monopolar electric pulses and whistler mode waves, *Geophys. Res. Lett.*, *25*, 4117-4120, 1998.

S. R. Bounds and C. A. Kletzing, 203 Van Allen Hall, Department of Physics and Astronomy, University of Iowa, Iowa City, IA 52242. (srb@gamma.physics.uiowa.edu; craig-kletzing@uiowa.edu)

R F. Pfaff, Mail Code 696, NASA Goddard Space Flight Center, Greenbelt, MD 20771 (rob.pfaff@gsfc.nasa.gov).

S. F. Knowlton, Physics Department, Auburn University, Auburn, AL 36830.

F. S. Mozer and M. A. Temerin, Space Sciences Laboratory, University of California at Berkeley, Berkeley, CA 94720.

(Received April 20, 1999; revised June 23, 1999;
accepted June 24, 1999.)